
Towards Automated Circuit Discovery for Mechanistic Interpretability

Arthur Conmy^{†*}, Augustine N. Mavor-Parker^{‡*}, Aengus Lynch^{‡*},
Stefan Heimersheim[§], Adrià Garriga-Alonso^{†*}

[†]Independent

[‡]University College London

[§]Institute of Astronomy, University of Cambridge

Abstract

Recent work in mechanistic interpretability has reverse-engineered nontrivial behaviors of transformer models. These contributions required considerable effort and researcher intuition, which makes it difficult to apply the same methods to understand the complex behavior that current models display. At their core however, the workflow for these discoveries is surprisingly similar. Researchers create a data set and metric that elicit the desired model behavior, subdivide the network into appropriate abstract units, replace activations of those units to identify which are involved in the behavior, and then interpret the functions that these units implement. By varying the data set, metric, and units under investigation, researchers can understand the functionality of each neural network region and the circuits they compose. This work proposes a novel algorithm, Automatic Circuit Discovery (ACDC), to automate the identification of the important units in the network. Given a model’s computational graph, ACDC finds subgraphs that explain a behavior of the model. ACDC was able to reproduce a previously identified circuit for Python docstrings in a small transformer, identifying 6/7 important attention heads that compose up to 3 layers deep, while including 91% fewer the connections.

1 Introduction

Rapid progress in transformer language modelling (Vaswani et al., 2017; Devlin et al., 2019; OpenAI, 2023, *inter alia*) has directed attention towards understanding the causes of new capabilities (Wei et al., 2022) in these models. Researchers have identified precise high-level predictors of model performance (Kaplan et al., 2020), but transformers are still widely considered ‘black-boxes’ (Alishahi, Chrupała, and Linzen, 2019) like almost all other neural network models (Fong and Vedaldi, 2017; Buhrmester, Münch, and Arens, 2021).² Interpretability research aims to demystify machine learning models, for example by explaining model outputs in terms of domain-relevant concepts (Zhang et al., 2021).

Mechanistic interpretability refers to the reverse-engineering of model components into human-understandable algorithms (Olah, 2022). Much research in mechanistic interpretability focuses on **circuits** in machine learning models, defined as subsets of neural networks that use features across different layers (connected by weights) to implement interpretable algorithms (Olah et al., 2020). For example, in vision models, Cammarata et al. (2020) found circuits that detect curves, and Schubert et al. (2021) found circuits that detect image patches contrasting high- and low-frequency regions. More recently, in transformer models, Nanda et al. (2023) and Chughtai, Chan, and Nanda (2023) described how circuits for an algorithmic task gradually form throughout training. Wang et al. (2023) found a circuit that implements a high-level natural language task.

*Work partially done at Redwood Research. Correspondence to arthurconmy@gmail.com

²Though this perspective is not universal (Lipton, 2016).

In this work we use *computational subgraphs* of the neural network to represent circuits. Considering neural networks as computational graphs has led to better understanding of their components. For example, training dynamics in residual models can be explained by shallow paths through the computational graph (Veit, Wilber, and Belongie, 2016), MLP layers can be modelled as memory that is able to represent certain properties of the network inputs (Geva et al., 2021), and residual transformer models have been modelled as the sum of all different paths through the network (Elhage et al., 2021). Later work has used insights from looking at subgraphs of models in order to edit models’ behaviors (Bau et al., 2020; Meng et al., 2022) and test interpretability hypotheses (Chan et al., 2022).

The current approach to extracting computational subgraphs (such as circuits) from neural networks relies on a lot of manual inspection by humans (Räuker et al., 2022). This is a major obstacle to scaling up mechanistic interpretability to larger models and more behaviors. In this work we present an automatic method to extract computational graphs from neural networks, and explore the challenges and applications of automated interpretability.

Our main contributions are threefold. Firstly, we introduce Automatic Circuit Discovery (ACDC), a novel algorithm for finding important subgraphs in ML models (Section 3). Secondly, we find limitations of current existing work on finding sparse subsets of neural networks when we compare ACDC to both heuristic- and gradient-based methods (Michel, Levy, and Neubig, 2019; Cao, Sanh, and Rush, 2021, Section 4). Finally, we demonstrate how ACDC can automatically reproduce existing mechanistic interpretability results, and can provide a basis for novel research on circuits (Section 5).

2 Related work

Neural network pruning masks the weights of neural networks to make their connectivity more sparse (LeCun, Denker, and Solla, 1989). In contrast to our aims, the pruning literature is typically concerned with compressing neural networks for faster inference or to reduce storage requirements (Wang, Wohlwend, and Lei, 2020; Kurtic et al., 2022). Early work (Hassibi and Stork, 1992) hoped pruning would lead to more interpretable networks, but progress towards interpretability via pruning is limited (Grover, Gawri, and Manku, 2022). Further, the literature has historically focused on compressing computer vision architectures (Blalock et al., 2020) and here we focus on natural language processing (and in particular, transformers).

Pruned transformers are often constructed using gradient information. For example, Michel, Levy, and Neubig (2019) decide what heads should be pruned by the absolute value of their gradients, while “movement pruning” (Sanh, Wolf, and Rush, 2020) removes parameters that have high velocity to a low magnitude. The Hessian matrix has also been used extensively to judge what parameters should be kept (LeCun, Denker, and Solla, 1989; Hassibi and Stork, 1992), with modern approaches

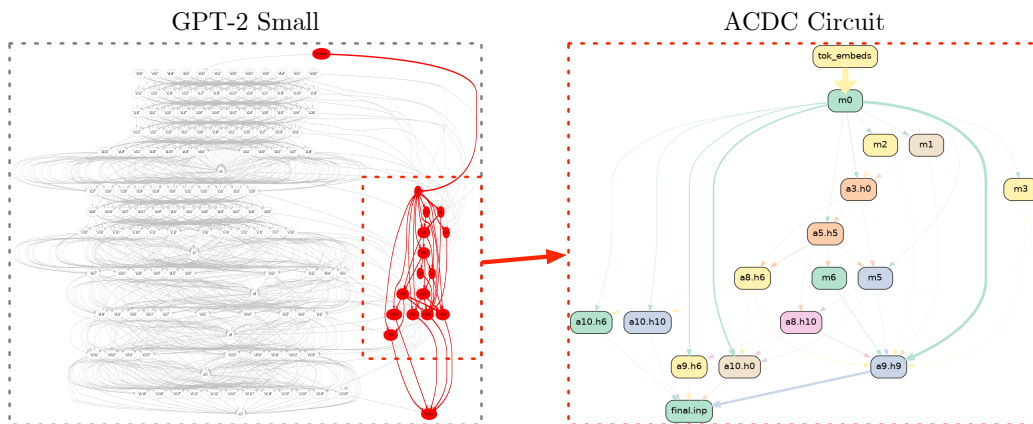


Figure 1: **Automatically discovering circuits with ACDC.** Left: the computational graph of GPT-2 Small with a recovered circuit for the IOI task in red. Right: the recovered circuit with labelled nodes. All heads recovered were identified as part of the IOI circuit (Wang et al., 2023).

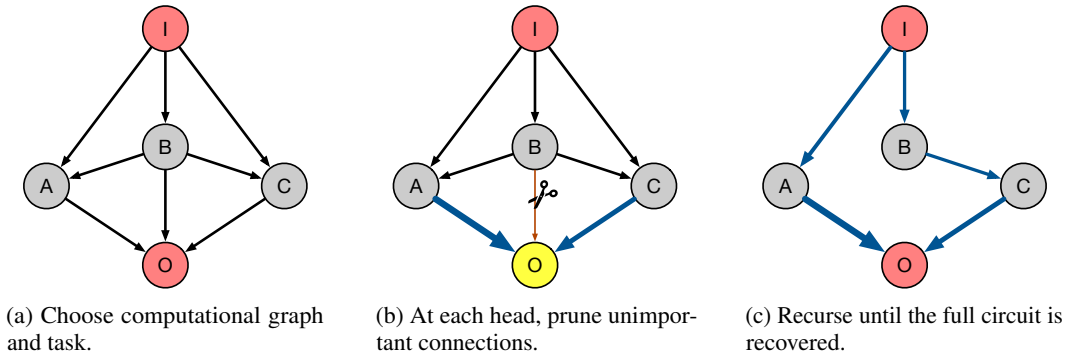


Figure 2: **How ACDC works** (Steps 2a-2c). Step 2a: a practitioner specifies a computational graph of the model, the task they want to investigate, and a threshold under which to remove connections. Step 2b: ACDC iterates over nodes in the computational graph, replacing activations of connections between a node and its children, and measuring the effect on the output metric. Connections are removed if their measured effect on the metric under corruption is below the threshold τ . Step 2c: recursively apply Step 2b to the important nodes found by previous times we performed Step 2b. The ACDC procedure returns a subgraph of the original computational graph.

using approximations that avoid the prohibitive cost of computing the Hessian for large language models (Wang, Wohlwend, and Lei, 2020; Kwon et al., 2022; Frantar and Alistarh, 2023). Lastly, techniques that prune small weights have been used as a baseline (Sanh, Wolf, and Rush, 2020) and have proven to be competitive for transformers (Han et al., 2015; Kurtic and Alistarh, 2022).

Masks can also be learned from data, with an objective function that juggles model performance and network sparsity (Louizos, Welling, and Kingma, 2018; Wang, Wohlwend, and Lei, 2020; Cao, Sanh, and Rush, 2021, Section 4.2). This is a useful comparison as unlike many pruning algorithms, ACDC and learnable masks prune in “one-shot” (Frantar and Alistarh, 2023), meaning that we do not change the weights of our model after pruning. Furthermore, learnable methods are a suitable comparison because they can prune whole layers and heads rather than masking individual weight parameters.

Causal interpretation. Much prior research on understanding language models has drawn inspiration from causal inference (Pearl, 2009), leading to the development of frameworks that provide causal explanations for model outputs (Pearl, 2009; Feder et al., 2021; Geiger et al., 2021; Wu et al., 2021). Other work Vig et al. (2020) discusses the difference between indirect effects and direct effects inside language models, and experiments on removing subsets of these heads using heads’ direct effects as proxies for the overall contribution of these heads. Goldowsky-Dill et al. (2023) introduce ‘path patching’ to analyze the effects of different subsets of edges in computational graphs of models. They also use a ‘treeify’ operation to consider all possible paths through a residual neural network.

Saliency maps are a visualization technique commonly used for automatic interpretation of the behavior of neural networks in both computer vision (Simonyan, Vedaldi, and Zisserman, 2014) and natural language processing (Li et al., 2016). Saliency maps highlight features *in the input data* that contribute most to a model’s predictions. Common methods for generating saliency maps include gradient-based methods (Ancona et al., 2018), occlusion-based methods (Ribeiro, Singh, and Guestrin, 2016) as well as model-specific approaches (Brocki and Chung, 2019). The methods described can produce useful high-level visualizations of how neural networks compute output distributions conditioned on their input (Goferman, Zelnik-Manor, and Tal, 2010). However, the visualizations produced are sometimes independent of the labels attached to training datapoints (Adebayo et al., 2018) and can also be insensitive to changes in inputs that are intuitively important (Sundararajan, Taly, and Yan, 2017).

3 Methodology

In the previous section, we discussed how some existing work uses causal interventions to understand particular model behaviors, and other works rewrite computational graphs of models to understand model internals. In this section we explain our novel algorithm, Automatic Circuit Discovery (ACDC;

see Algorithm 1 and Figure 2), that uses causal interventions to elucidate the key model internals for particular tasks models perform. There are three components to the algorithm: the **space of circuits** we search over (Section 3.1), how we go about **evaluating circuits** (Section 3.2) and the **search algorithm** used to select the circuit (Section 3.3).

3.1 The space of circuits

Consider a computational graph G with input node I and output node O , such as the graph in Figure 2a (which we use as a running example).

Following Wang et al. (2023), we define a *circuit* in a model as a subgraph of its computational graph G , and we search over this space of subgraphs. All edges not present in the computational graph are considered unimportant for the current task. Hence we set these edge’s values their activation on a corrupted input (see Section 3.2). Additionally, we only consider subgraphs where all nodes and edges lie on a paths to O as it is unclear how to interpret other subgraphs. For a given machine learning model there are several computational graphs that define its computation. For example, the subgraphs can include individual neurons that the model uses, or merely includes MLPs as its nodes. In our work we fix a particular computational graph before running ACDC on it.

Many previous works search over the space of subsets of model components or parameters (Cao, Sanh, and Rush, 2021; Michel, Levy, and Neubig, 2019; Vig et al., 2020). Our work considers a hypothesis space that is considerably larger, since it considers the mediating effect components have on later components. For example, in Figure 2c the component C has no direct path on the output, but it does have an effect through A on the output.

Building from Elhage et al. (2021), other researchers have considered searching over the space of all subsets of paths in a network (called the ‘treeified’ network (Goldowsky-Dill et al., 2023)). Our subspace of circuits is less expressive than this. It is unclear how to optimize over this intractably large space of hypotheses (there are over 10^{14} paths through the attention heads and MLPs in GPT-2 small, for example), though this is an interesting future research direction.

3.2 Evaluating circuits

Given a subgraph H of a computational graph (Section 3.1), we need a way to evaluate its performance on a particular task. In this section we define how we evaluate circuits and provide an example of a circuit that we evaluate.

We define a task by a dataset on which H can be evaluated and a dataset of corrupted inputs on which the task is not present. Then we define $H(x_i, x'_i)$ as the result of setting all edges not present in H to their activation on x'_i (a corrupted input). This defines $H(x_i, x'_i)$, the output probability distribution of the subgraph under such an experiment. Finally we evaluate H by computing the KL divergence $D_{KL}(G(x_i)||H(x_i, x'_i))$ between the model and the subgraph’s predictions. We let $D_{KL}(G||H)$ denote the average KL divergence over a set of datapoints. Using KL divergence instead of (for example) the probability that the subgraph places on the correct completion means that we can’t achieve better performance than the model itself. Appendix A discusses this overperformance issue further.

As an example, Elhage et al. (2021) use sequences including repeated tokens ($x_i = \dots AB\dots AB$, where A and B are distinct tokens) to find induction heads (Section 4.2) that predict the correct next token. In our induction experiments, we set x'_i equal to a sentence that does not have any repeated tokens.

3.3 The search algorithm

In Section 3.1 we described how our space of circuits is all the subgraphs of a computational graph. In Section 3.2 we described how to evaluate these subgraphs given a task of interest, and in this section we describe how we search over this space. We will validate that this approach recovers circuits that reflect the mechanisms inside models in Section 4. We refer the reader to Figure 5 and Algorithm 1 throughout the explanation for pedagogical reasons.

Informally, a run of ACDC iterates in reverse (topological) order through the computational graph G , starting at the output node. At every node, it attempts to remove as many edges that enter this node as

possible such that the KL divergence between the subgraphs and the model do not increase that much. Finally, once all nodes are iterated over, the algorithm (when successful) recovers a graph that i) is far sparser than the original graph and ii) recovers good performance on the task. Section 4 evaluates how ACDC compares by these metrics to other methods.

The ACDC algorithm has one hyperparameter τ , the threshold. We describe the algorithm in the notation of Section 3.2 in the pseudocode in Algorithm 1. We use a reverse topological sort routine so that nodes are processed from the output node back to the input node, and nodes are always processed before their inputs. We do not specify the order in which we iterate over the parents w of v . By default our implementation left this iterating from later-layer heads to earlier-layer heads. The order of the parents sometimes affects experimental results (Appendix C).

Algorithm 1: The ACDC algorithm.

Data: Computational graph G , dataset $(x_i)_{i=1}^n$, corrupted datapoints $(x'_i)_{i=1}^n$ and threshold τ .

Result: Subgraph $H \subseteq G$.

```

1  $H \leftarrow G$  // Initialize H to the full computational graph
2  $H \leftarrow H.reverse\_topological\_sort()$  // Sort H so output first
3 for  $v \in H$  do
4   for  $w$  parent of  $v$  do
5      $H_{new} \leftarrow H \setminus \{w \rightarrow v\}$ 
6     if  $D_{KL}(G||H_{new}) - D_{KL}(G||H) < \tau$  then
7        $H \leftarrow H \setminus \{w \rightarrow v\}$  // Remove the unimportant edge
8     end
9   end
10 end
11 return  $H$ 

```

4 Validation

To validate the ACDC algorithm’s use for interpreting neural networks, we conduct experiments to answer the following questions. When ACDC finds a subgraph of the computational graph of a neural network

- **Q1:** does ACDC identify the subgraph corresponding to the underlying algorithm implemented by the neural network?
- **Q2:** does ACDC avoid including components which do not participate in the elicited behavior?

We use two toy tasks to study these questions: simple `tracr` algorithms (where we have a ground truth of how the neural networks implement each task) in Section 4.1, and the task of induction in natural language in a 2-layer transformer in Section 4.2.

In Section 4.1, we study algorithms that can be converted into transformer weights using the `tracr` compiler (Lindner et al., 2023). This allows us to confirm that ACDC can recover subgraphs that implement the algorithms that neural networks encode, since `tracr` provides a ‘white-box’ implementation of the internal computation, unlike gradient descent. This means there is a ground-truth for validating our interpretability tool. We confirm both **Q1** and **Q2** in this case.

In Section 4.2, we study the induction (Elhage et al., 2021) task in a toy, two-layer transformer trained by gradient descent. In this case there is not a ‘ground truth’ circuit that implements induction. Therefore we measure the KL divergence and the number of edges in subgraphs that ACDC recovers across a range of thresholds. In some settings, almost all Pareto-optimal³ subgraphs are found by ACDC (Figure 4a). However, other methods perform as well in a different setting (Figure 4b).

³A subgraph is Pareto-optimal if it is not Pareto-dominated by any other subgraphs. A subgraph H is Pareto-dominated if there exists a different subgraph with at most the KL divergence of H and at most the number of edges of H .

4.1 Faithfulness to algorithmic tasks with `tracr`

To check whether ACDC identifies the subgraph corresponding to a neural network’s underlying algorithm (**Q1**), we use examples from the `tracr` library (Lindner et al., 2023). `tracr` compiles RASP programs (Weiss, Goldberg, and Yahav, 2021) into the weights of transformers. RASP programs are a subset of all the functions that transformers can implement. An example of a function that can be represented in the RASP programming language is the `frac_prevs` function. Given an input string s , the `frac_prevs` function computes the proportion of characters equal to a given fixed character (for example, x) at each position in s . In this section we use the `frac_prevs` task to confirm **Q1** and **Q2** and then discuss how our work generalizes to more RASP programs.

We firstly check that the `frac_prevs` transformer has an algorithm which ACDC can reverse-engineer (**Q1**). We generate a computational graph with nodes for every neuron in the computation from the transformer generated by `tracr`. We then set the corrupted datapoints $(x'_i)_{i=1}^n$ to a random permutation of the clean datapoints and set the threshold⁴ $\tau = 0.1$. The results are in Figure 3b. ACDC recovers exactly the component of the outputs of MLP 1 and Attention Head 2 that are used to compute the proportions of x at each place in the output, including the Q-, K- and V-composition with Attention Head 2. This results in 0 KL divergence from the model’s outputs, which shows that the answer to **Q1** in this case is yes.

We next examine whether any other components of the transformer are recovered by ACDC when applied to the `frac_prevs` task, addressing **Q2**. As shown in Figure 3b, there are no extra nodes present. In fact, this computational graph visualization produced by ACDC is more compact than the complete view of the states of the residual stream, as illustrated in Figure 3a (from Lindner et al. (2023)). In this case, the transformer is small enough for a practitioner to study each individual state in the forward pass. However, for larger transformers this would be intractable, which necessitates the use of different interpretability tools. Section 5 discusses several use cases of ACDC on larger transformers trained on more diverse datasets.

We provide an additional example of ACDC applied to a task from the `tracr` library in Appendix B, which also satisfies **Q1** and **Q2**. However, the most crucial applications of ACDC, as described in Section 5, involve cases where ground-truth access to the implemented algorithm is unavailable. Consequently, it is essential to study ACDC in models trained using gradient descent rather than those compiled with `tracr`.

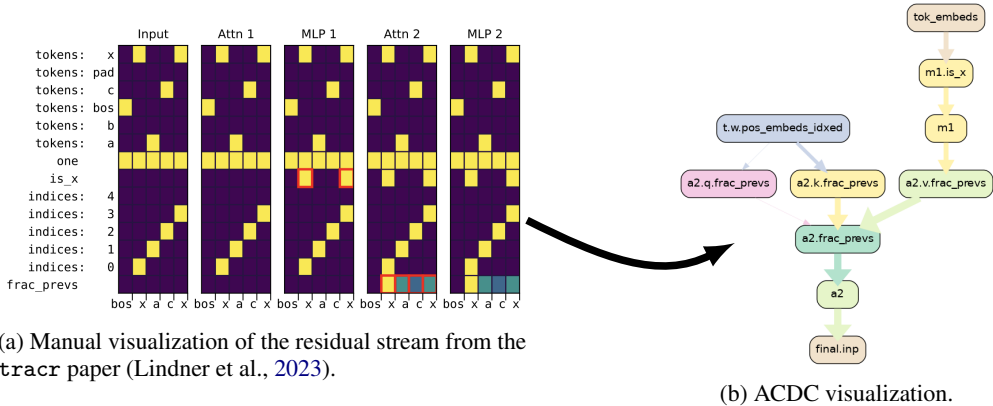


Figure 3: Two visualizations of how a `tracr`-compiled transformer completes the `frac_prevs` task.

4.2 Comparison to baseline on induction in a small transformer

We have established that ACDC recovers the true circuit in a simple task where the ground truth is known (in Section 4.1 above). However, the `tracr` setting is far from realistic: for example, most of the weights of the compiled transformer are zero. In this section, we provide further evidence for **Q1** and **Q2**, by studying the induction task (Elhage et al., 2021) in a small transformer. Specifically, we

⁴Any threshold $\tau > 0$ recovers the subgraph. We also randomize the positional embeddings of corrupted datapoints. Both details are discussed in Appendix B.

explain how we compare two existing methods to ACDC (Section 4.2.1), explain our experimental setup (Section 4.2.2) and evaluate the performance of ACDC compared to Subnetwork Probing (Section 4.2.3 and Figure 4).

4.2.1 Alternative Techniques

Subnetwork Probing (Cao, Sanh, and Rush, 2021, SP) prunes model weights with an objective that combines accuracy and sparsity (Louizos, Welling, and Kingma, 2018). SP aims to retain enough information such that a probe can still extract linguistic information from the model’s hidden states. To ensure a fair comparison to ACDC, we adapt the implementation in the following ways (see Appendix C.1 for more details):

1. We do not train a probe.
2. We change the objective of their optimization process from the loss to the KL divergence between the masked model and the base model.
3. We generalize the masking technique so we can replace activations with both zero activations and corrupted activations.

Head Importance Score for Pruning (HISP) is a method introduced by Michel, Levy, and Neubig (2019) to efficiently prune individual attention heads. HISP ranks the heads by importance scores I_h (Appendix C.2) and prunes all the heads except those with the top k scores. We measure the KL divergence and calculate the number of edges for each value of k in order to compare HISP with ACDC and SP. Like SP, this method only considers replacing head activations with zero activations, and therefore we once more introduce a generalization to replacement with corrupted activations (for details, see Appendix C.2).

4.2.2 Experimental Protocol

We use 40 sequences of 300 tokens from a filtered validation set of OpenWebText (Gokaslan et al., 2019). The filter removes validation examples that do not contain examples of induction — subsequences of the form " A, B, \dots, A, B ", where A and B are distinct tokens. We only measure KL divergence for the model’s predictions of the second B tokens in all examples of the subsequences A, B, \dots, A, B . We use both zero activations and corrupted activations to compare ACDC and SP. To use ACDC with zero activations, we apply one change to the procedure described in Section 3: instead of setting activations of edges not present in the subgraph to the activations on a corrupted dataset, we set their value equal to 0. We describe how we adapt the methods from Section 4.2.1 to be used with both zero activations and corrupted activations in Appendix C.1 for SP and Appendix C.2 for HISP.

We used 21 thresholds for ACDC, logarithmically spaced between 10^{-2} and $10^{0.5}$ inclusive. We ran SP with hand-picked thresholds that led to a diversity of outputs (see Appendix C). We ran HISP for all values of k up to the total number of nodes in the transformer’s computational graph. The results are found in Figure 4.

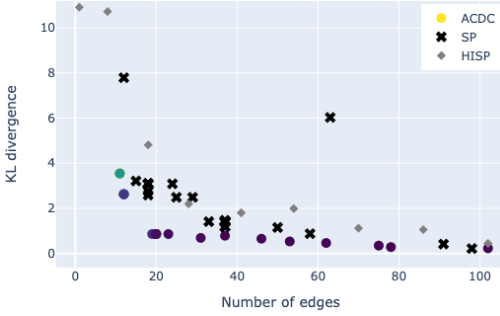
4.2.3 Evaluation of Results

When we compared the subgraphs produced by the three methods with zero activation replacements in Figure 4a, we found that 15/19 of the Pareto-optimal subgraphs were found by ACDC. HISP found Pareto-optimal subgraphs with 1 and 8 edges, and SP found Pareto-optimal subgraphs with 18 and 98 edges, but all other 15 Pareto-optimal subgraphs were found by ACDC.

However, when we used corrupted activations rather than zero activations (Figure 4b), SP and ACDC both generated 42.9% (9/21) of the Pareto-optimal subgraphs. HISP only recovered three of the Pareto-optimal subgraphs. In this case, the gradient-descent method appears to have explored the space of subgraphs as effectively than ACDC.

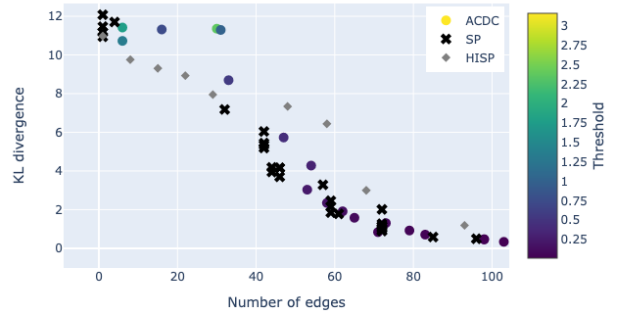
Surprisingly, all three methods recovered subgraphs with lower KL divergence when zero activations were used rather than corrupted activations. It is unclear why the methods achieve better results with corruptions that are likely to be more destructive. A possible explanation is that there are ‘negative’ components in models that are detrimental to the tasks, and the zero activations are more disruptive to these components. A discussion of how methods could be adjusted to deal with this difficulty can be found in Alternative 2 in Appendix A.

Pruning with zero activations



(a) Comparison of methods with zero activations.

Pruning with corrupted activations



(b) Like Figure 4a, but with corrupted activations.

Figure 4: Comparison of ACDC and SP with both zero activations (Figure 4a) and corrupted activations (Figure 4b).

A further problem is that we used KL divergence as a proxy for the faithfulness of the subgraphs, though this metric may not reflect whether the subgraphs found complete the induction task in the same way as the model. Empirically, there is some evidence that ACDC did recover the important components of the induction circuit (Figure 8), which strengthens the case for **Q1**. However, other components are found in addition to the mainline induction circuitry, which means there is not further evidence for **Q2**. In Section 5, we compare ACDC with two prior works that recovered circuits in models. This allows us to test more directly whether ACDC recovers the subgraphs that carry out the task inside the model.

5 Scaling ACDC

In Section 4 we validated the ACDC algorithm on transformers that contained ground truth circuits (Section 4.1) and on the induction task (Section 4.2). In this section, we test ACDC on harder tasks in more realistic models. The tasks that we study are the completion of particular docstrings (Heimersheim and Janiak, 2023) in Subsection 5.1, the Indirect Object Identification (IOI) circuit in GPT-2 small (Wang et al., 2023) in Subsection 5.2 and the completion of correct gendered pronouns (Mathwin et al., 2023) in Subsection 5.3. We find that ACDC can perform better on KL divergence metrics than existing interpretability work, be useful at different levels of granularity and reveal interpretable components that input-output based techniques such as saliency maps could not find. We also highlight limitations of ACDC in each of these cases to help inform future research.

All three tasks in this section study next-token prediction in language models. We use small datasets of synthetic examples of similar sentences and completions. An example of one sentence from each dataset is shown in Table 1. Further details of the models, tasks and the exact ACDC setup can be found in Appendices D-F.

Section	Prompt	Completion
5.1	<pre>def function(self, files, obj, state, size, shape, option): """document string example :param state: performance analysis :param size: pattern design :param</pre>	shape
5.2	When John and Mary went to the store, Mary gave a bottle of milk to	John
5.3	So Sarah is a really nice person, isn't	she

Table 1: The three next-token completion tasks in Section 5. Additional experimental details can be found in Appendices D-F.

Metric	Full model	ACDC LD	ACDC KL	Manual heads	Manual circuit
Mean logit diff.	0.48	0.18	-2.4	-1.2	-3.9
Correct-fraction	64%	44%	12%	42%	0%
Edges	1377	90	34	388	26

Table 2: Comparing our ACDC docstring results to manual interpretation from Heimersheim and Janiak (2023) using their metrics. We compare (from left to right) the full model, the subgraph from ACDC runs optimizing for logit difference (LD), and KL divergence (KL), as well as the subgraphs made manually from the attention heads given in Heimersheim and Janiak (2023) and finally the manual circuit that the work found. The metrics used are (a) mean logit difference between the correct variable name and the highest wrong variable name, and (b) the fraction of test cases where the model assigned a higher logit to the right answer than to any of the 5 wrong answers.

5.1 The docstring circuit

Heimersheim and Janiak (2023) find a circuit in a small language model that is responsible for completing python docstrings, such as the prompt shown in Table 1. This circuit of attentions heads controls which variable the model predicts in each docstring line, e.g in Table 1 it chooses shape over obj, state, size, or option. The circuit consists of 5 main attention heads, composing in up to three stages.

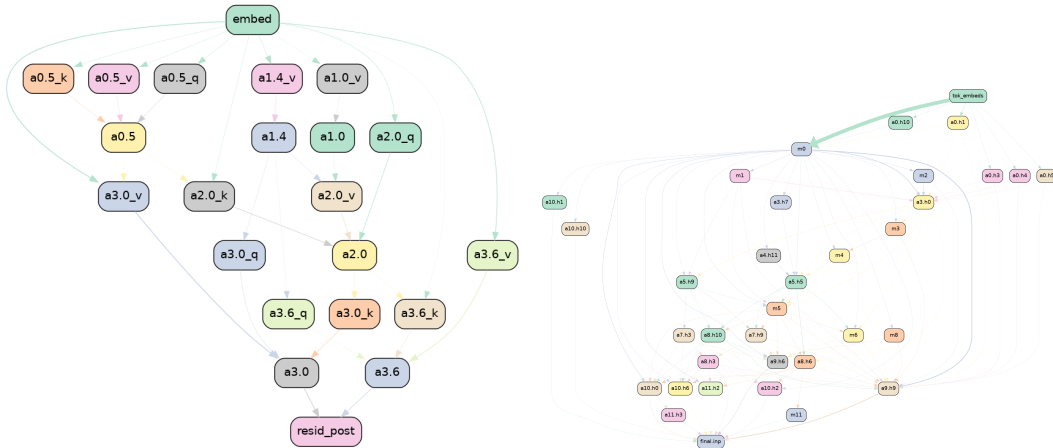
We apply the ACDC algorithm (Section 3) to their dataset and generate the subgraph shown in Figure 5a. Comparing this the original circuit Heimersheim and Janiak, 2023 we find (a) overlapping heads, (b) heads found by ACDC only, and (c) heads found in the manual interpretation only. In the first class (a) we find heads 0.5, 1.4, 2.0, 3.0, and 3.6. All these manually identified heads are recovered by ACDC. In class (b) we find head 1.0 which the authors later add to their circuit to improve performance (Heimersheim and Janiak, 2023), ACDC shows for the first time where this head belongs in the circuit. In class (c) we find heads 0.2, 0.4 and 1.2. However, the first two heads are not actually relevant under the docstring distribution and only added by the authors manually. Head 1.2 is considered a non-essential but supporting head by the authors and not identified by ACDC at the current threshold.

We compare the numerical results between the ACDC circuit (34 edges) and the circuit described in Heimersheim and Janiak (2023) in Table 2. The authors run a simple test including only their heads but not specifying edges (this corresponds to 388 edges), as well as suggest a 26-edge circuit without being able to test it. Since Heimersheim and Janiak (2023) use logit difference as their metric, we add a second ACDC run (90 edges) to the comparison that optimizes logit difference rather than KL divergence (see Appendix A for details on this adjustment). The corresponding subgraph can be found in Figure 9. ACDC achieves similar or better performance in both metrics used by Heimersheim and Janiak (2023) while—as expected—being much more specific (i.e. using fewer edges).

A limitation worth noting is that we applied ACDC to a computational graph of attention heads and their query, key and value computational nodes, while Heimersheim and Janiak (2023) considered the attention heads outputs into every token position separately. This allowed them to distinguish two functions fulfilled by the same attention head (layer 1, head 4) at different positions, which couldn’t be inferred from the output of ACDC alone. We make this choice for performance reasons (the long sequence length would have made the experiments significantly slower) but this is not a fundamental limitation. In Section 5.3 we use ACDC to isolate the effects of individual positions in a different task.

5.2 The IOI circuit

Wang et al. (2023) find a circuit ‘in the wild’ in GPT-2 small (Radford et al., 2019). The circuit identifies indirect objects (see for example Table 1) by using several classes of attention heads. In this subsection we analyze how successful ACDC’s circuit recovery (Figure 1) is. All nine heads found in Figure 1 belong to the IOI circuit, which is a subset of 26 heads out of a total of 144 heads in GPT-2 small. Additionally, these 9 heads include heads from three different classes (Previous Token Heads, S-Inhibition Heads and Name Mover Heads) that are sufficient to complete the IOI task, showing that ACDC indeed can recover circuits rather than just subgraphs.



(a) ACDC Subgraph on the docstring task, $\tau = 0.095$.

(b) ACDC on the IOI task, $\tau = 0.03$.

Figure 5: Two examples on running ACDC on different tasks (Section 5). Thresholds τ are given in the captions.

However, Figure 1 does not include heads from all the head classes that Wang et al. (2023) found, as it does not include the Negative Name Mover Heads or the Previous Token Heads. In Figure 5b we run ACDC with a lower threshold and find that it does recover Previous Token Heads. Despite using a lower threshold, the subgraph still does not recover Negative Name Mover Heads, and the reduced threshold results in the identification of numerous less significant heads. This is a case where KL divergence is insufficient for approximating model performance. When circuit components are important but harmful for model performance, ACDC may remove these components in order to decrease the KL divergence. We think that this limitation represents an important direction for future empirical and theoretical work. For example, we think that the following questions are open:

- To what extent do negative components arise in transformer language models?
- What are better metrics for measuring how well interpretations including negative components reflect model performance?

We discuss some modifications to ACDC that partially address these issues in Appendix A.

5.3 Gendered pronoun completion

Mathwin et al. (2023) begin to elicit the subgraph of GPT-2 small responsible for correctly gendered pronouns in GPT-2 small. They used an earlier version of ACDC as the basis of ongoing work (see Appendix F for full details). The result of applying ACDC with a low threshold $\tau = 0.05$ is shown in Figure 11.

The computational subgraphs generated by ACDC on the gendered pronoun completion task (see Appendix F) show that MLP computations are more important than attention head computations in this task, compared to the IOI task (Section 5.2). Early, middle and late layer MLPs have important roles in the subgraph. For example, MLPs 3 and 5 are the important components at the name position (which must be used to identify the correct gender) as they have multiple incident edges, the MLP 7 at the ‘ is’ position has the most incoming connections of any node in the graph, and the late layer MLPs 10 and 11 have the largest direct effect on the output. MLP 7’s importance at the ‘ is’ position is an example of a discovery that could not have been made with more simple interpretability tools such as saliency maps (Section 2). This is because the ‘ is’ position *mediates* (Vig et al., 2020) the effect of the input position (which is before the ‘ is’ position) on the output position (which is after the ‘ is’ position).

6 Conclusion

We have identified a common workflow for mechanistic interpretability. First, pin down a behavior using a metric and data set. Second, conduct activation patching experiments to understand which

abstract units (e.g. transformer heads) are involved in the behavior. Third, iterate the previous steps with variations of the behavior under study, until the identified model behavior is understood.

The proposed algorithm, ACDC, systematically conducts all the activation patching experiments necessary to find which circuit composed of abstract units is responsible for the behavior. We have shown that ACDC recovers most of the compositional circuit which implements a given language model behavior, as judged by toy models where the implementation is known and comparison to previous mechanistic interpretability work. ACDC is also useful to produce *novel* mechanistic interpretability work, as demonstrated by Mathwin et al. (2023), which applied ACDC to discover the outline of a circuit for gendered pronoun completion (Section 5.3).

On balance, we think the evidence supports the claim that ACDC can automate part of interpretability work. However, the current algorithm has limitations which prevent it from fully automating the second step of the identified workflow (activation patching). First, it systematically misses some classes of abstract units that are part of the circuit, for example the negative name mover heads from IOI (Wang et al., 2023). Second, the behavior of the algorithm is sensitive to the iteration order of the search over abstract unit, which remains a hard to tune hyperparameter.

Another limitation of the current work is the lack of empirical justification for some of the design choices, such as the recommendation to use the KL divergence to specify the behavior. We leave an extensive exploration of valid design choices (ablation study), improving the limitations of the algorithm for future work.

Overall, this work is a step towards defining a paradigm for future mechanistic interpretability work. The paradigm is concrete enough to be partially automated, which we show by automating the discovery of both known and new language model behaviors. Automating mechanistic interpretability is likely necessary to be able to describe the many behaviors of the large models which are in use today, otherwise the amount of specialized labor required is prohibitive.

We hope that our open-source implementation of ACDC accelerates interpretability research from the community.

Acknowledgments and Disclosure of Funding

This work would not have been possible without the generous support of Redwood Research through their REMIX program. We would like to thank Chris Mathwin, Jett Janiak, Chris MacLeod, Neel Nanda and Alexandre Variengien for feedback on a draft of this paper. Arthur Conmy would like to thank Jacob Steinhardt, Alexandre Variengien and Buck Shlegeris for extremely helpful conversations that shaped ACDC. We would also like to thank Haoxing Du for working on an early tool, Daniel Ziegler who discussed experiments that inspired our Subnetwork Probing analysis, and Lawrence Chan who helped us frame our contributions and suggested several experiments. We provide two implementations of ACDC:⁵ one built on top of Redwood Research’s `rust_circuit` library (Garriga-Alonso et al., 2022) and one in the `transformer_lens` library (Nanda, 2022).

References

- Wang, Kevin Ro, Alexandre Variengien, Arthur Conmy, Buck Shlegeris, and Jacob Steinhardt (2023). “Interpretability in the Wild: a Circuit for Indirect Object Identification in GPT-2 Small”. In: *The Eleventh International Conference on Learning Representations*. URL: <https://openreview.net/forum?id=NpsVSN6o4u1>.
- Vaswani, Ashish, Noam Shazeer, Niki Parmar, Jakob Uszkoreit, Llion Jones, Aidan N. Gomez, Lukasz Kaiser, and Illia Polosukhin (2017). *Attention Is All You Need*. arXiv: 1706.03762 [cs.CL].
- Devlin, Jacob, Ming-Wei Chang, Kenton Lee, and Kristina Toutanova (2019). *BERT: Pre-training of Deep Bidirectional Transformers for Language Understanding*. arXiv: 1810.04805 [cs.CL].
- OpenAI (2023). *GPT-4 Technical Report*. arXiv: 2303.08774 [cs.CL].

⁵Both implementations are available at <https://github.com/ArthurConmy/Automatic-Circuit-Discovery>

- Wei, Jason, Yi Tay, Rishi Bommasani, Colin Raffel, Barret Zoph, Sebastian Borgeaud, Dani Yogatama, Maarten Bosma, Denny Zhou, Donald Metzler, Ed H. Chi, Tatsunori Hashimoto, Oriol Vinyals, Percy Liang, Jeff Dean, and William Fedus (2022). *Emergent Abilities of Large Language Models*. arXiv: 2206.07682 [cs.CL].
- Kaplan, Jared, Sam McCandlish, Tom Henighan, Tom B. Brown, Benjamin Chess, Rewon Child, Scott Gray, Alec Radford, Jeffrey Wu, and Dario Amodei (2020). *Scaling Laws for Neural Language Models*. arXiv: 2001.08361 [cs.LG].
- Alishahi, Afra, Grzegorz Chrupała, and Tal Linzen (2019). “Analyzing and interpreting neural networks for NLP: A report on the first BlackboxNLP workshop”. In: *Natural Language Engineering* 25.4, pp. 543–557. DOI: 10.1017/S135132491900024X.
- Fong, Ruth C. and Andrea Vedaldi (2017). “Interpretable Explanations of Black Boxes by Meaningful Perturbation”. In: *IEEE International Conference on Computer Vision, ICCV 2017, Venice, Italy, October 22-29, 2017*. IEEE Computer Society, pp. 3449–3457. DOI: 10.1109/ICCV.2017.371. URL: <https://doi.org/10.1109/ICCV.2017.371>.
- Buhrmester, Vanessa, David Münch, and Michael Arens (2021). “Analysis of Explainers of Black Box Deep Neural Networks for Computer Vision: A Survey”. In: 3.4, pp. 966–989. ISSN: 2504-4990. DOI: 10.3390/make3040048. URL: <https://www.mdpi.com/2504-4990/3/4/48>.
- Lipton, Zachary C. (2016). *The Mythos of Model Interpretability*. URL: <https://arxiv.org/abs/1606.03490>.
- Zhang, Yu, Peter Tiño, Aleš Leonardis, and Ke Tang (2021). “A survey on neural network interpretability”. In: 5.5, pp. 726–742. DOI: 10.1109/TETCI.2021.3100641.
- Olah, Chris (2022). *Mechanistic Interpretability, Variables, and the Importance of Interpretable Bases*. <https://www.transformer-circuits.pub/2022/mech-interp-essay>.
- Olah, Chris, Nick Cammarata, Ludwig Schubert, Gabriel Goh, Michael Petrov, and Shan Carter (2020). “Zoom In: An Introduction to Circuits”. In: *Distill*. DOI: 10.23915/distill.00024.001.
- Cammarata, Nick, Shan Carter, Gabriel Goh, Chris Olah, Michael Petrov, Ludwig Schubert, Chelsea Voss, Ben Egan, and Swee Kiat Lim (2020). “Thread: Circuits”. In: <https://distill.pub/2020/circuits>. DOI: 10.23915/distill.00024.
- Schubert, Ludwig, Chelsea Voss, Nick Cammarata, Gabriel Goh, and Chris Olah (2021). “High-Low Frequency Detectors”. In: *Distill*. DOI: 10.23915/distill.00024.005.
- Nanda, Neel, Lawrence Chan, Tom Lieberum, Jess Smith, and Jacob Steinhardt (2023). “Progress measures for grokking via mechanistic interpretability”. In: *The Eleventh International Conference on Learning Representations*. URL: <https://openreview.net/forum?id=9XFSbDPmdW>.
- Chughtai, Bilal, Lawrence Chan, and Neel Nanda (2023). *A Toy Model of Universality: Reverse Engineering How Networks Learn Group Operations*. URL: <https://arxiv.org/abs/2302.03025>.
- Veit, Andreas, Michael J. Wilber, and Serge J. Belongie (2016). “Residual Networks Behave Like Ensembles of Relatively Shallow Networks”. In: *Advances in Neural Information Processing Systems 29: Annual Conference on Neural Information Processing Systems 2016, December 5-10, 2016, Barcelona, Spain*. Ed. by Daniel D. Lee, Masashi Sugiyama, Ulrike von Luxburg, Isabelle Guyon, and Roman Garnett, pp. 550–558. URL: <https://proceedings.neurips.cc/paper/2016/hash/37bc2f75bf1bcfe8450a1a41c200364c-Abstract.html>.
- Geva, Mor, Roei Schuster, Jonathan Berant, and Omer Levy (2021). “Transformer Feed-Forward Layers Are Key-Value Memories”. In: *Proceedings of the 2021 Conference on Empirical Methods in Natural Language Processing*. Association for Computational Linguistics, pp. 5484–5495. DOI: 10.18653/v1/2021.emnlp-main.446. URL: <https://aclanthology.org/2021.emnlp-main.446>.
- Elhage, Nelson, Neel Nanda, Catherine Olsson, Tom Henighan, Nicholas Joseph, Ben Mann, Amanda Askell, Yuntao Bai, Anna Chen, Tom Conerly, Nova DasSarma, Dawn Drain, Deep Ganguli, Zac Hatfield-Dodds, Danny Hernandez, Andy Jones, Jackson Kernion, Liane Lovitt, Kamal Ndousse, Dario Amodei, Tom Brown, Jack Clark, Jared Kaplan, Sam McCandlish, and Chris Olah (2021). “A Mathematical Framework for Transformer Circuits”. In: *Transformer Circuits Thread*. URL: <https://transformer-circuits.pub/2021/framework/index.html>.
- Bau, David, Steven Liu, Tongzhou Wang, Jun-Yan Zhu, and Antonio Torralba (2020). *Rewriting a Deep Generative Model*. URL: <https://arxiv.org/abs/2007.15646>.
- Meng, Kevin, David Bau, Alex J Andonian, and Yonatan Belinkov (2022). “Locating and editing factual associations in GPT”. In: *Advances in Neural Information Processing Systems*.
- Chan, Lawrence, Adria Garriga-Alonso, Nix Goldowsky-Dill, Ryan Greenblatt, Jenny Nitishinskaya, Ansh Radhakrishnan, Buck Shlegeris, and Nate Thomas (2022). *Causal scrubbing: A*

- method for rigorously testing interpretability hypotheses*. Alignment Forum. URL: <https://www.alignmentforum.org/posts/JvZhhzycHu2Yd57RN/causal-scrubbing-a-method-for-rigorously-testing>.
- Räuker, Tilman, Anson Ho, Stephen Casper, and Dylan Hadfield-Menell (2022). *Toward Transparent AI: A Survey on Interpreting the Inner Structures of Deep Neural Networks*. URL: <https://arxiv.org/abs/2207.13243>.
- Michel, Paul, Omer Levy, and Graham Neubig (2019). “Are Sixteen Heads Really Better than One?” In: *Advances in Neural Information Processing Systems 32: Annual Conference on Neural Information Processing Systems 2019, NeurIPS 2019, December 8-14, 2019, Vancouver, BC, Canada*. Ed. by Hanna M. Wallach, Hugo Larochelle, Alina Beygelzimer, Florence d’Alché-Buc, Emily B. Fox, and Roman Garnett, pp. 14014–14024. URL: <https://proceedings.neurips.cc/paper/2019/hash/2c601ad9d2ff9bc8b282670cdd54f69f-Abstract.html>.
- Cao, Steven, Victor Sanh, and Alexander Rush (2021). “Low-Complexity Probing via Finding Subnetworks”. In: *Proceedings of the 2021 Conference of the North American Chapter of the Association for Computational Linguistics: Human Language Technologies*. Association for Computational Linguistics, pp. 960–966. DOI: [10.18653/v1/2021.naacl-main.74](https://doi.org/10.18653/v1/2021.naacl-main.74).
- LeCun, Yann, John Denker, and Sara Solla (1989). “Optimal brain damage”. In: 2.
- Wang, Ziheng, Jeremy Wohlwend, and Tao Lei (2020). “Structured Pruning of Large Language Models”. In: *Proceedings of the 2020 Conference on Empirical Methods in Natural Language Processing (EMNLP)*. Association for Computational Linguistics, pp. 6151–6162. DOI: [10.18653/v1/2020.emnlp-main.496](https://doi.org/10.18653/v1/2020.emnlp-main.496). URL: <https://aclanthology.org/2020.emnlp-main.496>.
- Kurtic, Eldar, Daniel Campos, Tuan Nguyen, Elias Frantar, Mark Kurtz, Benjamin Fineran, Michael Goin, and Dan Alistarh (2022). “The optimal BERT surgeon: Scalable and accurate second-order pruning for large language models”. In: 5.
- Hassibi, Babak and David Stork (1992). “Second order derivatives for network pruning: Optimal brain surgeon”. In: 5.
- Grover, Jasdeep Singh, Bhavesh Gawri, and Ruskin Raj Manku (2022). “DeepCuts: Single-Shot Interpretability based Pruning for BERT”. In: 5.
- Blalock, Davis W., Jose Javier Gonzalez Ortiz, Jonathan Frankle, and John V. Guttag (2020). “What is the State of Neural Network Pruning?” In: *Proceedings of Machine Learning and Systems 2020, MLSys 2020, Austin, TX, USA, March 2-4, 2020*. Ed. by Inderjit S. Dhillon, Dimitris S. Papailiopoulos, and Vivienne Sze. mlsys.org. URL: <https://proceedings.mlsys.org/book/296.pdf>.
- Sanh, Victor, Thomas Wolf, and Alexander M. Rush (2020). “Movement Pruning: Adaptive Sparsity by Fine-Tuning”. In: *Advances in Neural Information Processing Systems 33: Annual Conference on Neural Information Processing Systems 2020, NeurIPS 2020, December 6-12, 2020, virtual*. Ed. by Hugo Larochelle, Marc’Aurelio Ranzato, Raia Hadsell, Maria-Florina Balcan, and Hsuan-Tien Lin. URL: <https://proceedings.neurips.cc/paper/2020/hash/ea15aaba768ae4a5993a8a4f4fa6e4-Abstract.html>.
- Kwon, Woosuk, Sehoon Kim, Michael W Mahoney, Joseph Hassoun, Kurt Keutzer, and Amir Gholami (2022). “A Fast Post-Training Pruning Framework for Transformers”. In: *arXiv preprint arXiv:2204.09656*.
- Frantar, Elias and Dan Alistarh (2023). *SparseGPT: Massive Language Models Can Be Accurately Pruned in One-Shot*.
- Han, Song, Jeff Pool, John Tran, and William Dally (2015). “Learning both weights and connections for efficient neural network”. In: *Advances in neural information processing systems* 28.
- Kurtic, Eldar and Dan Alistarh (2022). “GMP*: Well-Tuned Global Magnitude Pruning Can Outperform Most BERT-Pruning Methods”. In: *arXiv preprint arXiv:2210.06384*.
- Louizos, Christos, Max Welling, and Diederik P. Kingma (2018). “Learning Sparse Neural Networks through L_0 Regularization”. In: *6th International Conference on Learning Representations, ICLR 2018, Vancouver, BC, Canada, April 30 - May 3, 2018, Conference Track Proceedings*. OpenReview.net. URL: <https://openreview.net/forum?id=H1Y8hhg0b>.
- Pearl, Judea (2009). *Causality. Models, Reasoning, and Inference*. 2nd ed. Cambridge University Press. ISBN: 978-0-521-89560-6. DOI: [10.1017/CB09780511803161](https://doi.org/10.1017/CB09780511803161).
- Feder, Amir, Nadav Oved, Uri Shalit, and Roi Reichart (2021). “CausaLM: Causal Model Explanation Through Counterfactual Language Models”. In: 47.2, pp. 333–386. DOI: [10.1162/coli_a_00404](https://doi.org/10.1162/coli_a_00404). URL: <https://aclanthology.org/2021.cl-2.13>.
- Geiger, Atticus, Hanson Lu, Thomas Icard, and Christopher Potts (2021). *Causal Abstractions of Neural Networks*. URL: <https://arxiv.org/abs/2106.02997>.

- Wu, Zhengxuan, Atticus Geiger, Josh Rozner, Elisa Kreiss, Hanson Lu, Thomas Icard, Christopher Potts, and Noah D. Goodman (2021). “Causal Distillation for Language Models”. arXiv:2112.02505. URL: <https://arxiv.org/abs/2112.02505>.
- Vig, Jesse, Sebastian Gehrmann, Yonatan Belinkov, Sharon Qian, Daniel Nevo, Simas Sakenis, Jason Huang, Yaron Singer, and Stuart Shieber (2020). *Causal Mediation Analysis for Interpreting Neural NLP: The Case of Gender Bias*. URL: <https://arxiv.org/abs/2004.12265>.
- Goldowsky-Dill, Nicholas, Chris MacLeod, Lucas Sato, and Aryaman Arora (2023). *Localizing Model Behavior with Path Patching*. arXiv: 2304.05969 [cs.LG].
- Simonyan, Karen, Andrea Vedaldi, and Andrew Zisserman (2014). *Deep Inside Convolutional Networks: Visualising Image Classification Models and Saliency Maps*. eprint: 1312.6034.
- Li, Jiwei, Xinlei Chen, Eduard Hovy, and Dan Jurafsky (2016). “Visualizing and Understanding Neural Models in NLP”. In: *Proceedings of the 2016 Conference of the North American Chapter of the Association for Computational Linguistics: Human Language Technologies*. Association for Computational Linguistics, pp. 681–691. DOI: 10.18653/v1/N16-1082. URL: <https://aclanthology.org/N16-1082>.
- Ancona, Marco, Enea Ceolini, Cengiz Öztireli, and Markus Gross (2018). “Towards better understanding of gradient-based attribution methods for Deep Neural Networks”. In: *6th International Conference on Learning Representations, ICLR 2018, Vancouver, BC, Canada, April 30 - May 3, 2018, Conference Track Proceedings*. OpenReview.net. URL: <https://openreview.net/forum?id=Sy21R9JAW>.
- Ribeiro, Marco Túlio, Sameer Singh, and Carlos Guestrin (2016). ““Why Should I Trust You?”: Explaining the Predictions of Any Classifier”. In: *Proceedings of the 22nd ACM SIGKDD International Conference on Knowledge Discovery and Data Mining, San Francisco, CA, USA, August 13-17, 2016*. Ed. by Balaji Krishnapuram, Mohak Shah, Alexander J. Smola, Charu C. Aggarwal, Dou Shen, and Rajeev Rastogi. ACM, pp. 1135–1144. DOI: 10.1145/2939672.2939778. URL: <https://doi.org/10.1145/2939672.2939778>.
- Brocki, Lennart and Neo Christopher Chung (2019). *Concept Saliency Maps to Visualize Relevant Features in Deep Generative Models*. eprint: 1910.13140.
- Goferman, Stas, Lihi Zelnik-Manor, and Ayellet Tal (2010). “Context-aware saliency detection”. In: *The Twenty-Third IEEE Conference on Computer Vision and Pattern Recognition, CVPR 2010, San Francisco, CA, USA, 13-18 June 2010*. IEEE Computer Society, pp. 2376–2383. DOI: 10.1109/CVPR.2010.5539929. URL: <https://doi.org/10.1109/CVPR.2010.5539929>.
- Adebayo, Julius, Justin Gilmer, Michael Muelly, Ian J. Goodfellow, Moritz Hardt, and Been Kim (2018). “Sanity Checks for Saliency Maps”. In: *Advances in Neural Information Processing Systems 31: Annual Conference on Neural Information Processing Systems 2018, NeurIPS 2018, December 3-8, 2018, Montréal, Canada*. Ed. by Samy Bengio, Hanna M. Wallach, Hugo Larochelle, Kristen Grauman, Nicolò Cesa-Bianchi, and Roman Garnett, pp. 9525–9536. URL: <https://proceedings.neurips.cc/paper/2018/hash/294a8ed24b1ad22ec2e7efea049b8737-Abstract.html>.
- Sundararajan, Mukund, Ankur Taly, and Qiqi Yan (2017). “Axiomatic Attribution for Deep Networks”. In: *Proceedings of the 34th International Conference on Machine Learning, ICML 2017, Sydney, NSW, Australia, 6-11 August 2017*. Ed. by Doina Precup and Yee Whye Teh. Vol. 70. Proceedings of Machine Learning Research. PMLR, pp. 3319–3328. URL: <http://proceedings.mlr.press/v70/sundararajan17a.html>.
- Lindner, David, János Kramár, Matthew Rahtz, Thomas McGrath, and Vladimir Mikulik (2023). “Tracr: Compiled Transformers as a Laboratory for Interpretability”. In.
- Weiss, Gail, Yoav Goldberg, and Eran Yahav (2021). “Thinking Like Transformers”. In: *Proceedings of the 38th International Conference on Machine Learning, ICML 2021, 18-24 July 2021, Virtual Event*. Ed. by Marina Meila and Tong Zhang. Vol. 139. Proceedings of Machine Learning Research. PMLR, pp. 11080–11090. URL: <http://proceedings.mlr.press/v139/weiss21a.html>.
- Gokaslan, Aaron, Vanya Cohen, Ellie Pavlick, and Stefanie Tellex (2019). *OpenWebText Corpus*. URL: <https://Skylion007.github.io/OpenWebTextCorpus>.
- Heimersheim, Stefan and Jett Janiak (2023). *A circuit for Python docstrings in a 4-layer attention-only transformer*. URL: <https://www.alignmentforum.org/posts/u6KXXmKFbXfWzoAXn/a-circuit-for-python-docstrings-in-a-4-layer-attention-only>.
- Mathwin, Chris, Guillaume Corlouer, Esben Kran, Fazl Barez, and Neel Nanda (2023). URL: <https://cmathw.itch.io/identifying-a-preliminary-circuit-for-predicting-gendered-pronouns-in-gpt-2-smal>.

- Radford, Alec, Jeff Wu, Rewon Child, David Luan, Dario Amodei, and Ilya Sutskever (2019). “Language Models are Unsupervised Multitask Learners”. In.
- Garriga-Alonso, Adrià, Nicholas Goldowsky-Dill, Ryan Greenblatt, Jenny Nitishinskaya, Radhakrishnan Ansh, Buck Shlegeris, Lexi Mattick, Fabien Roger, William Brandon, and Daniel M. Ziegler (2022). *Rust Circuit*. URL: https://github.com/redwoodresearch/rust_circuit_public.
- Nanda, Neel (2022). *TransformerLens*. URL: <https://github.com/neelnanda-io/TransformerLens>.
- Ramanujan, Vivek, Mitchell Wortsman, Aniruddha Kembhavi, Ali Farhadi, and Mohammad Rastegari (2020). “What’s Hidden in a Randomly Weighted Neural Network?” In: *2020 IEEE/CVF Conference on Computer Vision and Pattern Recognition, CVPR 2020, Seattle, WA, USA, June 13-19, 2020*. IEEE, pp. 11890–11899. DOI: [10.1109/CVPR42600.2020.01191](https://doi.org/10.1109/CVPR42600.2020.01191). URL: <https://doi.org/10.1109/CVPR42600.2020.01191>.
- Casper, Stephen, Yuxiao Li, Jiawei Li, Tong Bu, Kevin Zhang, and Dylan Hadfield-Menell (2023). *Benchmarking Interpretability Tools for Deep Neural Networks*. URL: <https://arxiv.org/abs/2302.10894>.
- Doshi-Velez, Finale and Been Kim (2017). *Towards A Rigorous Science of Interpretable Machine Learning*. arXiv: [1702.08608](https://arxiv.org/abs/1702.08608) [stat.ML].
- Jacovi, Alon and Yoav Goldberg (2020). *Towards Faithfully Interpretable NLP Systems: How should we define and evaluate faithfulness?* arXiv: [2004.03685](https://arxiv.org/abs/2004.03685) [cs.CL].

Appendix

A Alternatives to minimizing KL divergence

In the main text we presented ACDC as an algorithm that minimizes the KL divergence between the outputs of the model and a subgraph of the model (Section 3.2 and Algorithm 1). In this appendix we explain the modifications to ACDC that we will consider (Appendix A.1), and then review the effects of changing the metric (Appendix A.2) and changing the approach of extremizing a metric (Appendix A.3). Minimizing KL divergence was problematic because several existing works (Wang et al., 2023; Heimersheim and Janiak, 2023; Ramanujan et al., 2020) have found negative components that increase performance when ablated, and ACDC appears to not include these components (Section 5.2). The lack of standardized metrics for assessing the performance of algorithms in interpretability research is a long-standing challenge within the field (Casper et al., 2023) and the evaluation criteria that researchers use in practise have been widely criticized (Doshi-Velez and Kim, 2017; Jacovi and Goldberg, 2020; Lipton, 2016).

A.1 How to modify ACDC

The only line of Algorithm 1 that references KL divergence is Line 6, which has the condition

$$D_{KL}(G||H_{\text{new}}) - D_{KL}(G||H) < \tau \quad (1)$$

for the removal of an edge. All modifications to ACDC discussed in this Appendix replace Condition 1 with a new condition and do not change any other part of Algorithm 1. For example, if we wish to maximise the logit difference F between the circuit and a subgraph (Wang et al., 2023) in ACDC, we can change Condition 1 to⁶

$$F(H) - F(H_{\text{new}}) < \tau. \quad (2)$$

Appendix B gives another practical example of changing the metric from KL divergence. Implementations of all modifications to ACDC are provided at <https://github.com/ArthurConmy/Automatic-Circuit-Discovery>.

⁶We abuse notation so that $F(H)$ refers to some function of the outputs of H when ran on a dataset of example prompts, as in Section 3.2.

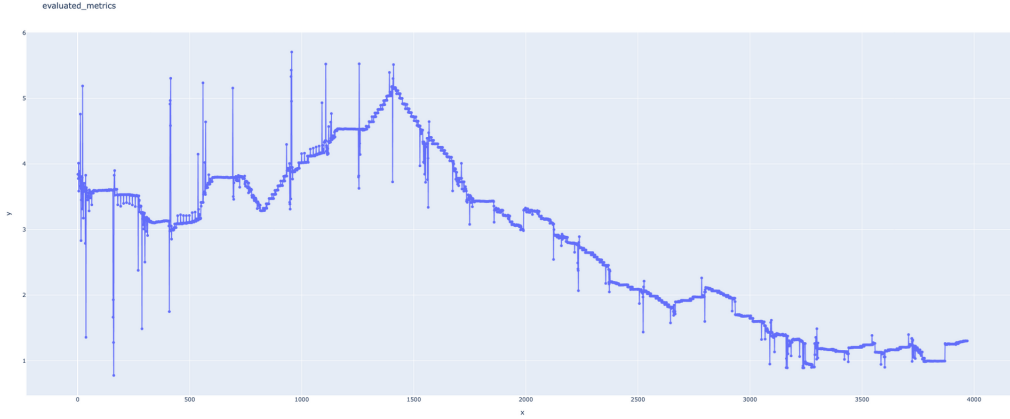


Figure 6: Plot of measure logit differences (y -axis) against time (x -axis) in a modified ACDC run. The large spikes are where an important edge is briefly removed, before being added back to the subgraph (Line 6 of Algorithm 1).

A.2 Alternatives to KL divergence

All three interpretability case studies in Section 5 originally used a variant of *logit difference* to measure the performance of subgraphs. Logit difference is the difference in logits for a correct output compared to a baseline incorrect output. Then, these works compare the distance between the logit difference of the circuit and the logit difference of the model. However, unlike KL divergence, this metric is not always positive — logit difference for a circuit could be larger or smaller than the logit difference of the model. We discuss issues that arise with this approach in Appendix A.3.

Beyond issues of non-negativity, logit difference can be problematic when we maximize it. For example, early experiments with Subnetwork Probing (Section 4.2) where we optimized for large logit difference rather than low KL divergence resulted in subgraphs that did not resemble the IOI circuit and had logit differences as large as 20.0. The IOI circuit has a logit difference of 3.0, and throughout the entirety of ACDC runs, logit difference is never larger than 7.0 (Figure 6). A logit difference of 20.0 represents a subgraph that places more than 10^9 times as much probability on the ‘John’ completion compared to the ‘Mary’ completion (Table 1), which seems far out of distribution from expected language model behavior, and didn’t provide an informative comparison to ACDC.

A.3 Alternatives to minimizing a metric

Two alternatives to minimizing a metric are to 1) match the model’s performance on a metric, or 2) only include edges that locally have a large effect. These could be formalised by the following alternatives to Condition 1, where F denotes any metric we could compute from a subgraph:

1. **Matching the model’s performance:** $|F(H_{\text{new}}) - F(G)| - |F(H) - F(G)| < \tau$.
2. **Only including locally large effects:** $|F(H_{\text{new}}) - F(H)| < \tau$.

Matching the model’s performance (also referred to as faithfulness by Wang et al. (2023)). Since KL divergence is always positive, Alternative 1 is identical to Condition 1 when F is the KL divergence between a subgraph’s outputs and the models’ outputs, but for metrics such as logit difference this represents a new optimization objective. Empirically we found that matching the model’s performance was unstable when we ran ACDC. For example, we ran a modified early version of ACDC that maximized the logit difference in the IOI circuit, and plotted the logit differences of subgraphs through the ACDC run (Figure 6). This shows that the logit difference of a subgraph could be as large as 5.0 and as low as 1.5 during a modified ACDC run. The IOI circuit has a logit difference of 3.55, and therefore the subgraph’s logit difference can be both larger and smaller than the model’s. This issue arises when the subgraph’s logit difference is larger than the model’s. In such cases, ACDC will discard model components that it would otherwise include when the subgraph’s logit difference is smaller than the model’s. This leads to inconsistencies between runs.

Only including locally large effects. Alternative 2 ignores the performance of the model G and instead focuses on changes that locally have a large effect. In principle, this would include negative heads, as they have a large magnitude effect in the opposite direction to the positive model components. However, we do not expect Alternative 2 to directly fix the problems identified in this Appendix. This is primarily because we don't optimize for an objective that can be measured for all subgraphs that ACDC iterates over and therefore there is no simple metric for the end performance of a subgraph recovered. This significantly complicates validation (Section 4) that ACDC can recover reliable subgraphs at all.

Overall, we found that KL divergence was the least flawed of all metrics we tried in this project, and think more practitioners should use it given i) the problems with other metrics listed, and ii) how empirically it can recover several circuits that were found by researchers using other metrics.

B More details on the `tracr` experiments

In this Appendix we discuss the experimental setup for the `tracr` experiment in Section 4.1, and an additional experiment from the `tracr` library.

B.1 Main text `tracr` experiment details

We used a transformer identical to the one studied in Lindner et al. (2023), and refer to that work for details on the `frac_prevs` task.

We make two modifications to the traditional ACDC setup. Firstly, we set the positional embeddings equal to randomized positional embeddings in the corrupted datapoints — otherwise, we don't recover any of the circuit components that depend only on positional embeddings (and not token embeddings). Secondly, since the output of this transformer is a real number r_i and not a probability distribution, we need to adapt our framework. Fortunately, considering each r_i a real random variable, we can define

$$D_{KL}(r_i||r'_i) := \begin{cases} 0 & \text{if } r_i = r'_i \\ \infty & \text{otherwise} \end{cases} \quad (3)$$

and then any threshold $\tau > 0$ recovers the circuit in Figure 3.

B.2 Another `tracr` experiment

To test ACDC on more than one example of a RASP program, we also used the 3-layer transformer that can reverse lists from the `tracr` Github implementation. Once more, the outputs of the transformer are not distributions so we use Equation 3 in cases where subgraph outputs do not match model outputs. We also randomize positional embeddings as in Appendix B.1 and recover a perfect circuit in Figure 7.

C More details on the induction experiments

Our induction experiments were performed on a 2-layer, 8-head-per-layer attention only transformer trained on OpenWebText (Gokaslan et al., 2019). The model is available in the TransformerLens (Nanda, 2022) library.⁷ We follow Appendix C of Goldowsky-Dill et al. (2023) for the construction of the dataset of induction examples.

The computational graph has a total of 305 edges, and in Figure 4 we only show subgraphs with at most 120 edges.

When iterating over the parents of a given node (Line 4 in Algorithm 1), we found that iterating in increasing order of the head index was important to achieve better results in Figure 4. Similar to all experiments in the work, we iterate in decreasing order of layers, so overall we iterate over head 1.0, then 1.1, ... then 1.7, then 0.0, then 0.1,

⁷The model can be loaded with `transformer_lens.HookedTransformer.from_pretrained(model_name = "redwood_attn_2l", center_writing_weights = False, center_unembed = False)`

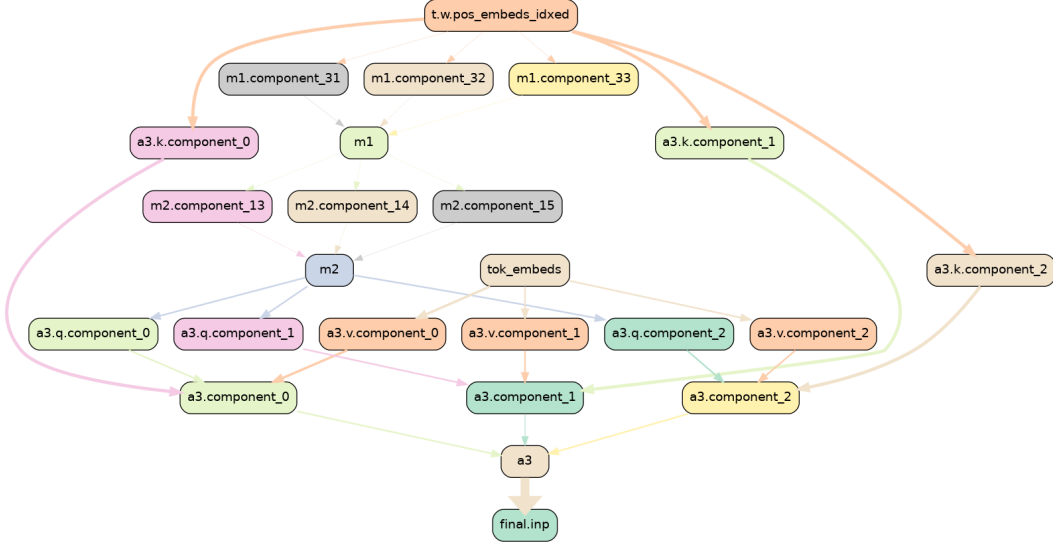


Figure 7: ACDC applied to reversing lists. This graph recovers perfect performance.

C.1 Subnetwork Probing

In Section 4.2.1 we described 3 modifications we made to Subnetwork Probing (Cao, Sanh, and Rush, 2021, SP). In this Appendix we provide more detail and motivation for these modifications:

1. **We do not train a probe.** ACDC does not use a probe and the mask that SP learns can be optimized without a probe.
2. **We change the objective of their optimization process from the loss to the KL divergence between the masked model and the base model.** ACDC uses the KL divergence to the model’s outputs (Algorithm 1) and so in order to compare the techniques in equivalent settings we also use the KL divergence for subnetwork probing.
3. **We generalize the masking technique so we can replace activations with both zero activations and corrupted activations.** Replacing activations with zero activations⁸ is useful for pruning (as they improve the efficiency of networks) but are not as commonly used in mechanistic interpretability (Goldowsky-Dill et al., 2023), so we adapt SP to use corrupted activations. SP learns a mask Z and then sets the weights ϕ of the neural network equal to $\phi * Z$ (elementwise multiplication). This means that outputs from attention heads and MLPs in models are scaled closer to 0 as mask weights are increased. To allow comparison with ACDC, we can linearly interpolate between a clean activation when the mask weight is 1 and a corrupted activation (i.e a component’s output on the datapoint x'_i , in the notation of Section 3.2) when the mask weight is 0.

The regularization coefficients λ (in the notation of Cao, Sanh, and Rush (2021)) we used were 0.01, 0.1, 10.0, 20.0, 40.0, 50.0, 55.0, 60.0, 65.0, 70.0, 80.0, 100.0, 120.0, 140.0, 160.0, 180.0, 200.0, 250.0, 300.0, 310.0, 320.0, 330.0, 350.0, 360.0, 370.0, 380.0, 400.0, 500.0, 600.0, 700.0, 800.0, 900.0 and 1000.0.

An example of a circuit found in the process is given in Figure 8. The number of edges for subgraphs found with Subnetwork Probing are computed by counting the number of edges between pairs of unmasked nodes.

C.2 Head Importance Score for Pruning

In Section 4.2.1 we compared ACDC with the Head Importance Score for Pruning (Michel, Levy, and Neubig, 2019, HISP). We borrow the author’s notation throughout this section, particularly from Section 4.1 and adapting it so it is this Appendix can be read after Section 3.

⁸Which is generally equivalent to setting weight parameters equal to 0.

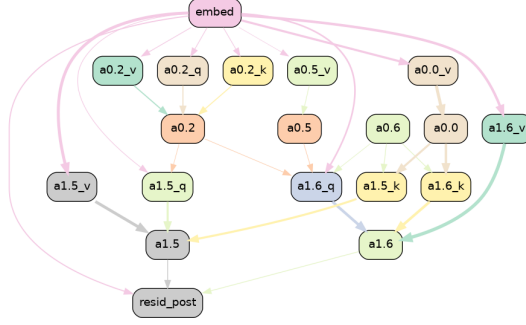


Figure 8: An example of a subgraph recovered by ACDC with corrupted activations and threshold $\tau = 0.5623$. This includes induction heads (1.5, 1.6) and a previous token head (0.0) as identified by Goldowsky-Dill et al. (2023).

The authors use masking parameters ξ_h for all heads, i.e scaling the output of each attention head by ξ_h , similar to the approach in Subnetwork Probing (Appendix C.1).

The authors define head importance as

$$I_h := \frac{1}{n} \sum_{i=1}^n \left| \frac{\partial \mathcal{L}(x_i)}{\partial \xi_h} \right|. \quad (4)$$

Since our work uses KL divergence rather than loss, we instead use the derivative of the KL divergence from the base model’s outputs.

Additionally, the authors only consider interpolation between clean and zero activations. In order to compare with corrupted activations, we can generalize ξ_h to be the interpolation factor between the clean head output $\text{Att}_h(x)$ (when $\xi_h = 1$) and the corrupted head output $\text{Att}_h(x')$ (when $\xi_h = 0$). In practice, this means that we compute I_h as

$$\frac{1}{n} \sum_{i=1}^n \left| (\text{Att}_h(x_i) - \text{Att}_h(x'_i))^T \frac{\partial \text{KL}}{\partial \text{Att}_h(x_i)} \right|. \quad (5)$$

To compute the importance for zero activations, we adjust Equation (5) so it just has a $\text{Att}_h(x)$ term, without the $\text{Att}_h(x')$ term. We also normalize all scores for different layers as in Michel, Levy, and Neubig (2019).

C.3 More details on Figure 4

The plots and all data of points within them can be found at https://github.com/ArthurConmy/Automatic-Circuit-Discovery/blob/acdc_tl/acdc/media/corrupted.json and https://github.com/ArthurConmy/Automatic-Circuit-Discovery/blob/acdc_tl/acdc/media/zero.json (and can be loaded from the plotly library).

D More details on the docstring experiments

D.1 Main text docstring circuit experiment details (Section 5.1)

We use the identical dataset to Heimersheim and Janiak (2023) in their accompanying Colab notebook.⁹ As corrupted dataset we use their `random_random` dataset that edits both the variable names in the function definition and in the docstring of prompts (Table 1).

We recomputed the correct-fraction percentage for the manual circuit in Heimersheim and Janiak (2023) but found it to be lower (30%) than what the authors reported (42%). We suspect that the

⁹Available at <https://colab.research.google.com/drive/17CoA1yARaWHvV14zQGcI3ISz1bIRZKS5> as of 8th April 2023

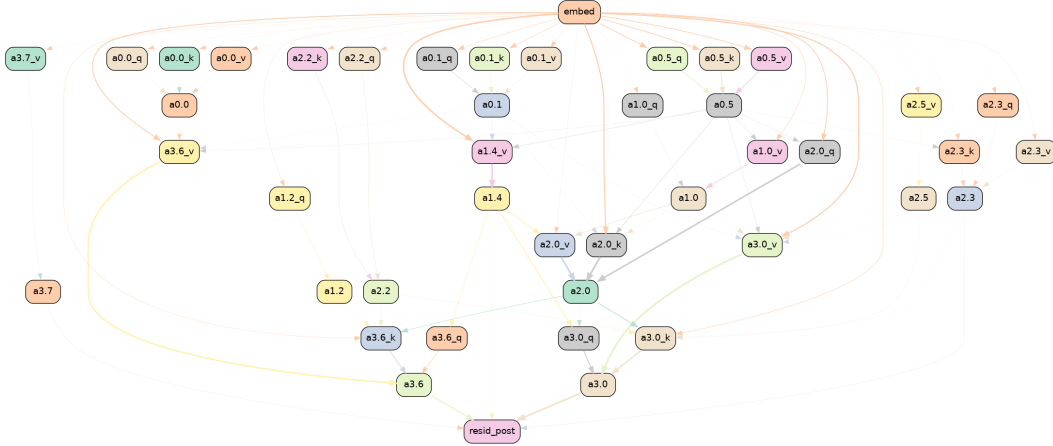


Figure 9: ACDC on docstring task maximizing logit difference ($\tau = 0.067$).

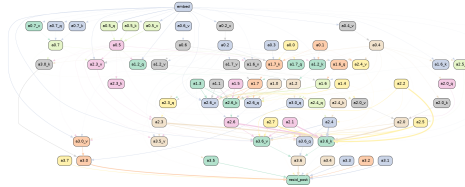


Figure 10: An ACDC run ($\tau = 0.067$) on the docstring circuit with zero activations.

original figure was miscomputed, though we report the larger percentage in Table 2 to be conservative in favour of the manual interpretation.

D.2 Additional docstring experiments

To compare ACDC more closely with the docstring work (Heimersheim and Janiak, 2023), we added an ACDC run with the objective to maximize the logit difference metric. We used a threshold of $\tau = 0.067$ and found the subgraph shown in Figure 9.

Unlike in the case of induction (Section 4.2), we found that replacing activations in the docstring circuit with zero activations led to far worse KL divergence than when corrupted activations were used. For example, with $\tau = 0.067$ (the same threshold that generated Figure 9) except with zero activations, we get the circuit Figure 10. This has 177 edges (Figure 9 has just 34), as well as a KL divergence of 3.35 and a logit difference of -2.895 . All these metrics are worse than the subgraph generated with corrupted activations (which had a KL divergence of 1.25).

E More details on the IOI experiments

In the ACDC run in Figure 1, we used a threshold of $\tau = 0.0575$. For ease of visualization, in the diagram on the left of Figure 1 we removed all edges between grey nodes more than 2 layers apart, and 90% of the edges between grey and red nodes.

Our IOI experiments were conducted with a dataset of $N = 50$ text examples from one template the IOI paper used (which can be found in Table 1). The corrupted dataset was examples from the ABC dataset (Wang et al., 2023) — for example ‘When Alice and Bob went to the store, Charlie gave a bottle of milk to’.

In the IOI experiments, we did not split the computational graph into the query, key and value calculations for each head. This enabled iteration to be faster, since subgraphs (e.g Figure 1) took 8 minutes to complete on a NVIDIA A100 GPU.



Figure 11: Gendered pronoun completion subgraph.

F More details on the gendered pronoun experiment

We used the dataset of $N = 100$ examples from Mathwin et al. (2023). The corrupted dataset was a set of prompts all the same as ‘That person is a really great friend, isn’t’ again the following the authors approach.

We defined a computational graph that split the attention heads query, key and value vectors by the sequence position they corresponded to. From the input sentence ‘So Sarah is a really nice person, isn’t’ we chose the tokens ‘Sarah’, ‘is’, ‘person’, ‘isn’ and ‘t’. We created more nodes in the computational graph for all other positions, but found that they were not used at all. The resulting subgraph can be found in Figure 11.

Figure 11 includes 74 of the 96250 connections in this computational graph (0.08%) and the KL divergence of 0.09 is 6% of the KL divergence (1.47) of the corrupted input from the model’s output.